

Article

Study on Facies Modeling of Tight Sandstone Reservoir Using Multi-Point Geostatistics Method Based on 2D Training Image—Case Study of Longdong Area, Ordos Basin, China

Naidan Zhang¹, Shaohua Li^{1,*} , Lunjie Chang², Chao Wang², Jun Li² and Bo Liang¹ ¹ School of Geosciences, Yangtze University, Wuhan 430100, China² Research Institute of Exploration and Development, Tarim Oilfield Company, CNPC, Korla 841000, China

* Correspondence: lish@yangtzeu.edu.cn

Abstract: The Longdong area in the Ordos basin is a typical fluvial reservoir with strong heterogeneity. In order to clarify the distribution law of underground reservoirs in the Longdong area, it is necessary to establish and optimize a 3D geological model to characterize the heterogeneity of reservoirs. This is of great significance for accelerating the exploitation of tight sandstone gas in the southwest of the Ordos basin. This study takes the P₂h₈ member of the Ct3 research area in the Longdong area as an example, analyzes the core and logging curve shape to divide the sedimentary microfacies, and establishes the facies model. In particular, in view of the difficulty in obtaining 3D training images under the existing conditions in the study area, we use the multi-point geostatistics method combining sequential two-dimensional condition simulation and the direct sampling method to establish the facies model. This method can simulate the 3D geological model by using the 2D training images composed of the digital plane facies diagrams and the well-connection facies diagrams. In addition, we choose the object-based method and sequential indicator method for comparative experiments to verify the feasibility of this method (sequential two-dimensional condition simulation combined with the direct sampling method) from many aspects. The results show that the multi-point geostatistics method based on 2D training images can not only match the well data, but also show the geometric characteristics and contact relationship of the simulation object. The distribution characteristics of sandbody thickness and modeling results are consistent with the actual geological conditions in the study area. This study explores the feasibility of this method in the 3D geological simulation of large-scale fluvial facies tight sandstone reservoirs. Additionally, it also provides a new idea and scheme for the modeling method of geologists in similar geological environments.

Keywords: Ordos Basin; tight sandstone gas reservoir; facies modeling; multi-point geostatistics; 2D training image



Citation: Zhang, N.; Li, S.; Chang, L.; Wang, C.; Li, J.; Liang, B. Study on Facies Modeling of Tight Sandstone Reservoir Using Multi-Point Geostatistics Method Based on 2D Training Image—Case Study of Longdong Area, Ordos Basin, China. *Minerals* **2022**, *12*, 1335. <https://doi.org/10.3390/min12101335>

Academic Editor: Behnam Sadeghi

Received: 10 August 2022

Accepted: 20 October 2022

Published: 21 October 2022

Publisher's Note: MDPI stays neutral with regard to jurisdictional claims in published maps and institutional affiliations.



Copyright: © 2022 by the authors. Licensee MDPI, Basel, Switzerland. This article is an open access article distributed under the terms and conditions of the Creative Commons Attribution (CC BY) license (<https://creativecommons.org/licenses/by/4.0/>).

1. Introduction

Tight sandstone gas is the main type of unconventional natural gas and plays an increasingly significant role in the energy structure [1,2]. Usually, the gas in a tight sandstone reservoir with a permeability of less than 0.1 mD and porosity of less than 10% can be referred to as tight (sandstone) gas [3]. Most scholars use N₂ and CO₂ adsorption experiments to obtain microscopic parameters of tight rock, including shale with a nano pore structure [4–6]. Because the occurrence state and migration mode of unconventional oil and gas are greatly different from those of conventional oil and gas, it brings gigantic challenges to oil and gas production [4,7]. The Asia Pacific and the Americas are the main regions where tight gas is distributed, accounting for more than 60% of the global total resources [7]. Large tight sandstone gas reserves have now been developed in the United States' San Juan basin and Canada's Elmworth basin [8]. China has also successively proved many tight sandstone gas reserves in the Ordos, Sichuan, Tarim, Songliao, and Bohai Bay basins, and the annual production of tight gas will reach 470 × 10⁸ m³ in 2020 [7,9]. The gas reservoir

in the eighth member of the Xiashihezi Formation (P₂h₈ member) of Permian in the Ordos Basin is the most successful example of tight sandstone gas exploration in China. At present, trillions of cubic meters of large tight sandstone gas reservoirs in Sulige, Wushenqi, and Yulin have been successfully explored and proven [10]. In recent years, natural gas exploration in the upper Paleozoic in the Ordos Basin has expanded southward. The P₂h₈ member in the Longdong area has now become a new area for natural gas exploration in the upper Paleozoic of the Ordos Basin [11,12]. Since the exploration of the tight sandstone gas reservoir in the Longdong area has only begun in recent years, its low well pattern density and low signal-to-noise ratio of seismic data make it difficult to effectively combine with logging data. Oil and gas field developers cannot meet the development needs due to their unclear understanding of underground geological conditions. Previous studies show that the P₂h₈ member in the Longdong area is a typical sandy braided river delta deposit [13,14]. Fluvial facies sand bodies are characterized by strong heterogeneity due to the frequent migration of river channels and multi-stage superposition in the process of sedimentation. In order to effectively reduce the risk of oil and gas exploration and development, there is an urgent need to use reservoir three-dimensional (3D) geological modeling technology to characterize reservoir heterogeneity and evaluate reservoir uncertainty [15,16].

There are numerous ways to perform 3D geological stochastic modeling, but they can be broadly classified into two types: One is object-based simulation and the other is pixel-based simulation. Among many methods, the methods used for the stochastic simulation of sedimentary facies mainly include marked point process, sequential indicator simulation (SIS), truncated Gauss, multi-point geostatistics (MPS), etc. [15–20]. Each random modeling method has its own applicability. The traditional modeling method has achieved good results in the simulation of sedimentary facies in some research areas, but it also has some limitations. At the same time, MPS has developed rapidly by combining the advantages of object-based and pixel-based methods. This method can better simulate highly heterogeneous fluvial reservoirs in practical applications and has been widely promoted and applied in recent years [21–24]. The key point of the multi-point geostatistical modeling method is to use a training image (TI) to show the distribution regularity of various parameters of the target reservoir in 3D space. How to obtain 3D TI is an important factor. Some scholars use the combination of well and earthquake and dissection in the dense well pattern area to restore the true situation of the reservoir [25–28]. However, high-quality seismic data are often only available in offshore oil fields, which can provide a good data basis for the study of TIs, so as to obtain a 3D TI that can reflect the characteristics of underground reservoirs [29]. Furthermore, the object-based method can be used to create the 3D TI. However, this method has limitations in producing TI with complex reservoir distribution rules and is difficult to show complex geological entities. In view of the difficulties in obtaining 3D TIs, many scholars try to directly use 2D TIs to build a 3D model.

Okabe used MPS based on 2D TIs to generate realistic 3D pore space to predict the multiphase flow in geological real porous media [30]. The actual underground geological spatial structure is complex, with certain continuity on the whole and unique characteristics in its parts. The underground situation is more heterogeneous. In order to realize the 3D construction of underground space structure attributes, Comunian proposed a sequential two-dimensional conditional simulation (s2Dcd) method [31]. This method can use two (or more) 2D TIs to reproduce complex geological patterns, which significantly improves the reconstruction of heterogeneous structures. The s2Dcd method has a good simulation effect when the conditional data are sparse. However, as the number of simulations increases and the conditional data become denser, the simulation effect will gradually decline. Direct sampling (DS) is a style-based multipoint modeling method proposed by Mariethoz and Renard in 2010 [32]. The DS method performs well when the conditional data are dense. However, due to the lack of limitations in the conditional data, the simulation performance of DS gradually deteriorates at locations remote from the conditional data. This method directly uses the similarity between data events to judge the simulation process. It can

increase target continuity and conserve computer memory because there is no need to create a search tree in advance. The DS can compensate for the s2dcd method's drawback, which is that when the conditional data are dense, the simulation target's continuity becomes worse due to too-strong restrictions. In 2017, Gueting used Mariethoz's improved DS algorithm combined with the s2Dcd method to conduct 3D simulations based on multiple 2D TIs [31–33]. This method combines the advantages and disadvantages of DS and s2Dcd in different simulation stages and improves the simulation effect of groundwater aquifer heterogeneity. In recent years, the 3D model construction technology based on 2D TI has achieved some application results in the field of MPS. The Longdong area is in the early stage of exploration, with low well pattern density and no high-precision seismic data. The distribution of underground sedimentary microfacies is unknown. Moreover, there is no comparable outcrop around the study area, so it is impossible to generate 3D TI by combining well and earthquake or object-based methods. It will be difficult and time-consuming for geologists to manually quantify the description based on the information on the well. However, the manual drawing of 2D TI is convenient and fast, and it can maximize geologists' geological knowledge and experience with similar sedimentary blocks. Finally, the 2D TI in line with geological knowledge is obtained. Existing approaches for simulating 3D geological models using 2D TIs are mostly used to simulate the microscopic digital core pore structure and are rarely used to simulate large-scale fluvial oil and gas reservoirs. This paper takes the Ct3 research area as an example. The facies modeling adopts the MPS method of s2Dcd combined with DS. This method uses the digital plane sedimentary facies map and vertical well connection profile as 2D TIs to simulate the 3D model.

This paper applies this method to the simulation of a fluvial tight sandstone gas reservoir. In order to verify this method and explore the feasibility of this method in the actual work area, we also chose the most widely used facies modeling methods, including the object-based method and the sequential indication method to establish sedimentary facies models [34]. We compare and analyze the advantages, disadvantages, and applicability of the above methods from many aspects. With the wide application of facies control modeling, the accuracy of its sedimentary facies model will directly affect the reliability of the whole model [3]. Therefore, the establishment and optimization of a fine 3D geological sedimentary facies model provides a basis for the subsequent reservoir physical property model. This paper aims to use the 2D TI to simulate the 3D model and also better represent the underground geological conditions and provide a new feasible idea and scheme for modeling under similar geological conditions.

2. Geological Setting

2.1. Structural and Stratigraphic Characteristics

The Ordos Basin is in central China, spanning the five provinces of Shaanxi, Gansu, Ningxia, Shanxi, and Mongolia, which covers an area of approximately 25×10^4 km² (Figure 1a) [3]. The Ordos Basin contains six tectonic units: Yimeng Uplift, Western Overthrust Belt, Tianhuan Depression, North Shanxi Slope, Western Shanxi Fold Belt, and Weibei Uplift (Figure 1b) [35]. It is a multistage cratonic basin. The main body of the Longdong area is situated on the North Shanxi slope, which is located in the southwest corner of the Ordos Basin. The structure is relatively stable [36,37]. The Ct3 study area is located in the Longdong area of the Ordos Basin. The Ct3 is approximately 1200 km². The upper Paleozoic in this area is divided into Carboniferous Benxi Formation(C₁b), Permian Taiyuan Formation(P₁t), Shanxi Formation(P₂s), Xiashihezi Formation(P₂h), Shangshihezi Formation(P₁h), and Shiqianfeng Formation(P₃q) from bottom to top. The main target stratum of the Ct3 study area is the P₂h₈ member (Figure 1c). According to the stratigraphic division law, the P₂h₈ member can be subdivided into four small beds from bottom to top: h₈¹, h₈², h₈³, and h₈⁴. The average thickness of each small bed is approximately 10 m. The average depth of the reservoir in the P₂h₈ member is 3744 m underground. The porosity is distributed between 4% and 10%, and the permeability is distributed between 0.08 and 1.0 mD. The P₂h₈ member in this area belongs to a tight sandstone reservoir.

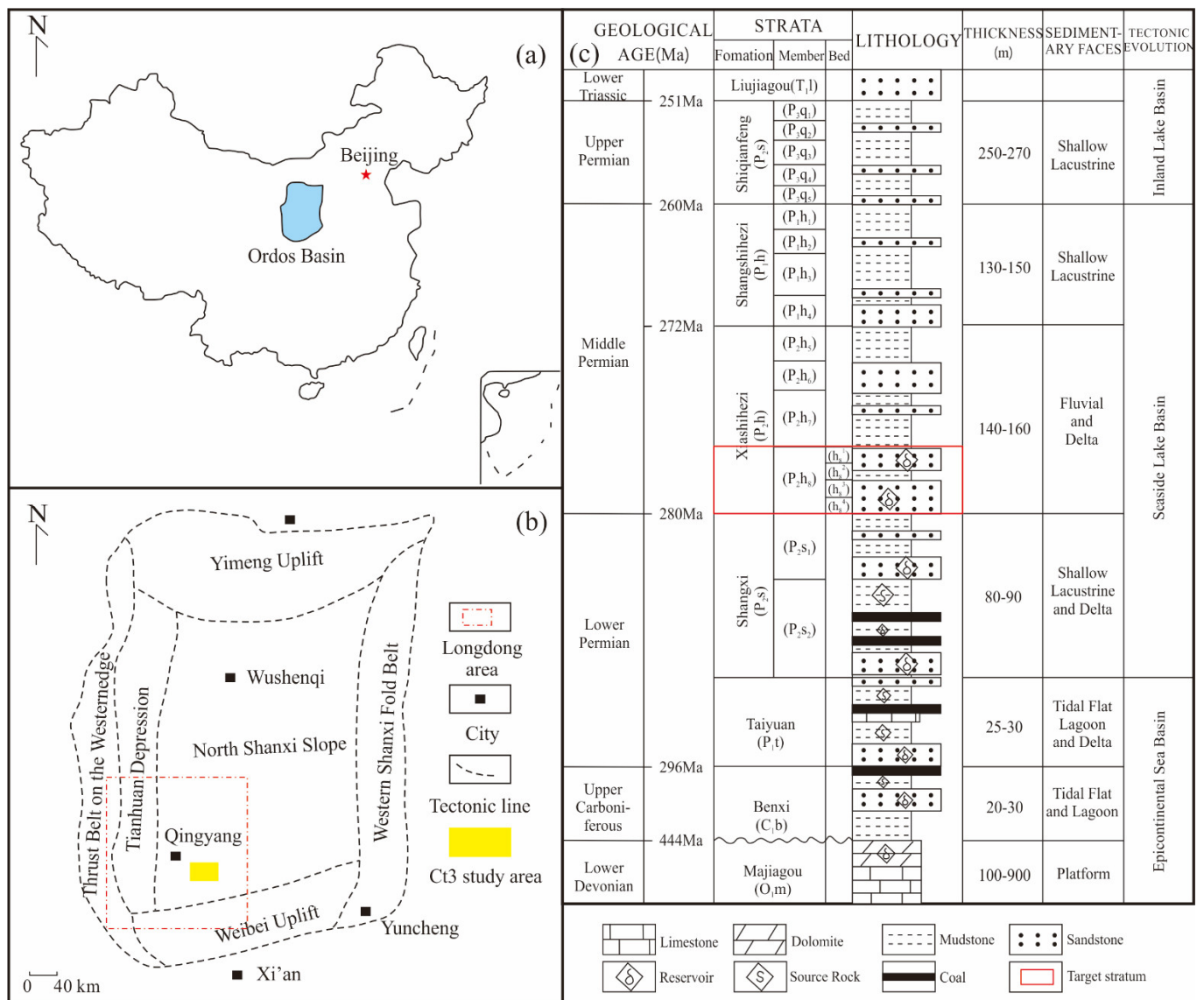


Figure 1. (a) Ordos Basin in China; (b) Ordos basin tectonic units and Longdong area; (c) sequence stratigraphic framework and sedimentary environment in Longdong area.

2.2. Characteristics of Sedimentary Microfacies

The Ct3 study area has 41 wells in total, including 8 coring wells. The average well spacing in the study area is 3000 m. All drilling wells have conventional logging curves with spontaneous potential (SP), gamma ray (GR), caliper log (CAL), acoustic (AC), neutron (CNL), density (DEN), true resistivity (RT), and induced conductivity (COND). These data are used to obtain the structural and stratigraphic framework and provide the basis for facies modeling. The total length of the P₂h₈ member cores sample is approximately 300 m. There are 634 core photos in the P₂h₈ member, which is particularly important for identifying the sedimentary microfacies in the study area. The sedimentary facies type of the P₂h₈ member in the Longdong area is a braided river delta, which has been the consensus of many scholars [14,38–40]. Identifying the type, color, and bedding structure of rocks from cores can directly recognize and preliminarily judge the sedimentary environment [41,42]. The reservoir sandstone of the P₂h₈ member is mainly composed of quartz sandstone and lithic quartz sandstone. Because the content of arkose is poor, it belongs to a high-energy environmental product far from the source [43]. It can be seen from the core obtained from the coring well that the sandstone is mainly gray and gray-white. The color of

mudstone is mainly gray, but there are also gray-white and variegated mudstones. The sandstone type is mainly gravelly coarse sandstone and coarse sandstone. The clastic particles are in sub-round to sub-angular shape, with medium to bad sorting. Parallel bedding and plate-like bedding are widely developed in sandstone. This indicates that the sediment is transported with the water flow for a long time and the hydrodynamic force is strong. In addition, plant root marks were found in the core, which revealed that the sedimentary environment was a semi-oxidation and semi-reduction shallow water environment. There is no collapse or diapir structure that marks the delta front in the core. Finally, it is comprehensively determined that the P₂h₈ member of the Ct3 study area is a braided river delta plain. According to the electro-facies' calibration, it is considered that there are three types of sedimentary microfacies in the area: Distributary channel, channel bar, and distributary interchannel. Figure 2 shows the division of sedimentary microfacies on a single well by taking well X in the study area as an example. The shape of the GR curve corresponding to the channel bar is a toothed and smooth box. The shape of the GR curve corresponding to the distributary channel is a toothed bell. The shape of the GR curve corresponding to the distributary interchannel is a toothed mudstone baseline. The established electrofacies template in this study area is applied to non-coring wells. The study of sedimentary facies is of guiding significance for the reasonable study of sandbody distribution. The researchers used heavy mineral analysis and clastic rock analysis to study the provenance of the Longdong area. According to the change rule of the mass fraction of heavy mineral components and their combination on the plane, it is found that the southwest of the Longdong area extends to the northeast with relatively "low zircon", "high quartz + rock debris", "low igneous rock debris", and "dolomite rock debris development", which generally reflects the southwest provenance characteristics. The results of the studies indicate that the provenance direction is to the southwest [39]. According to the principle of dominant facies, the sedimentary microfacies plan of the P₂h₈ member in the Ct3 study area is drawn in combination with the source direction (Figure 3).

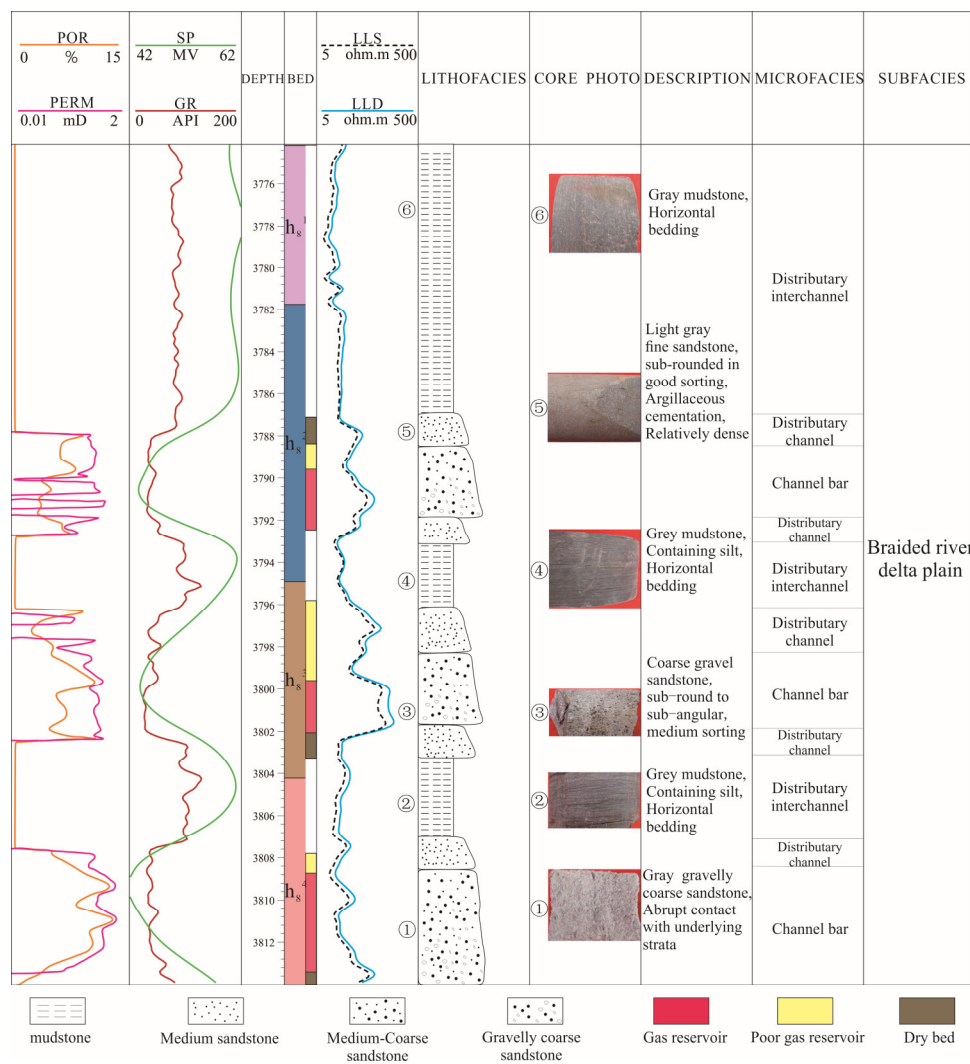


Figure 2. Comprehensive histogram of well X in Ct3 study area in P₂h₈ member.

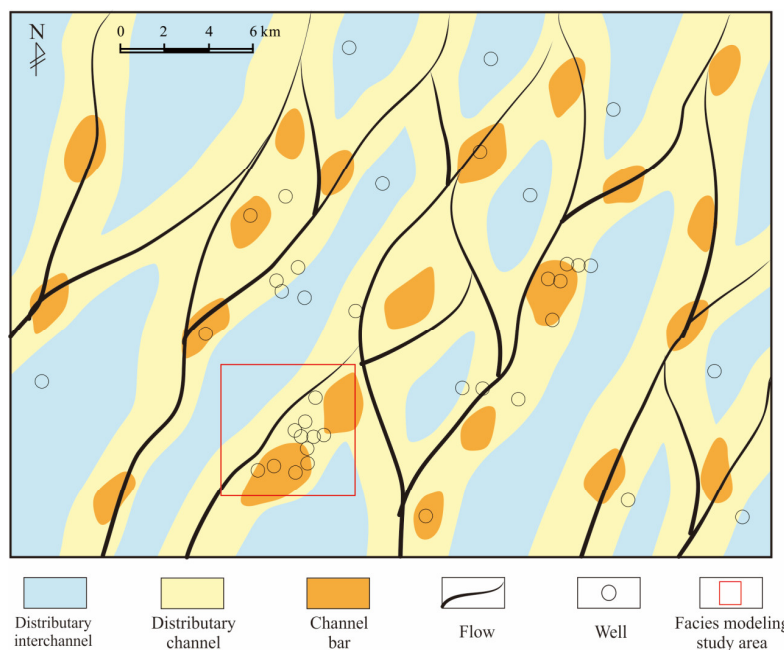


Figure 3. Distribution of plane sedimentary facies of P₂h₈ member in Ct3 study area.

3. Methods

The establishment of the facies model is used to establish corresponding facies models according to different methods after defining the types and distribution characteristics of sedimentary microfacies (Figure 4). The main process includes the following steps: (1) Import well data and establish a 3D structural model; (2) establish facies models by three different methods; (3) the facies models established by the three methods are compared and discussed according to various methods. Here, we use “Petrel” software to establish the structural model and the sedimentary facies model.

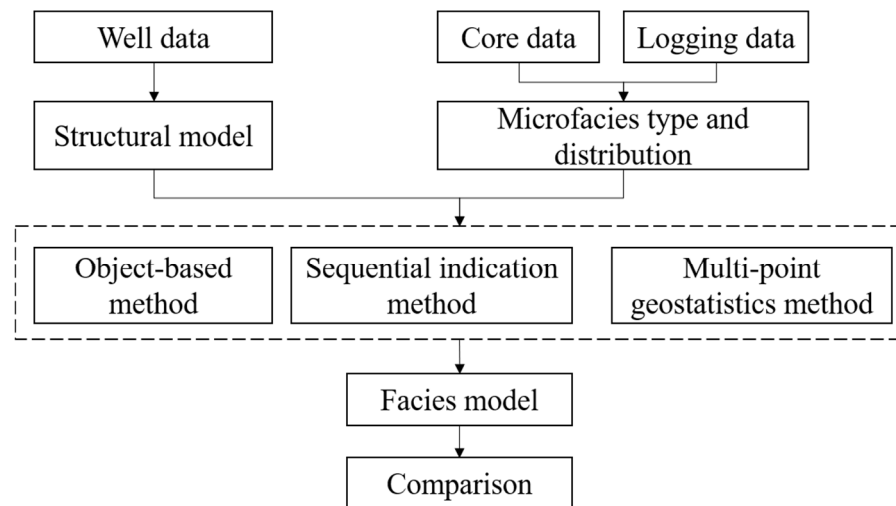


Figure 4. Workflow of creating facies model.

3.1. Geologic Structural Modeling

The Ct3 study area covers an area of approximately 1200 square kilometers. Because the area of Ct3 is too large and the computer simulation speed is limited, it is not suitable to simulate the whole study area. We select a small area (6 km × 6 km) with a relatively dense well pattern in Ct3 as the block of this facies modeling study, which includes 11 wells (Figure 3). The 3D model is composed of 100 layers longitudinally, and the vertical grid accuracy is 0.46 m. The horizontal grid size is 50 × 50 m. The number of grids in the I, J, and K directions is 120 × 120 × 100. The total number of grids is 144,000. This model (Figure 5a) represents the current structure of the P₂h₈ member in the study area. The topography of the structural model gradually increases from west to east, which is consistent with the relatively gentle west-dipping monocline structure in the Longdong area. The grid model of the geological structure can show the thickness of each bed (Figure 5b). The whole structural model also aptly represents the contact relationship between each sub layer in the vertical direction.

3.2. Facies Modeling

3.2.1. Object-Based Method

The object-based method takes the target object as the basic simulation unit, and needs to specify the shape, size, orientation, distribution, and other parameters of the simulated target. Through the study of target geometry, the target is directly generated in the modeling process. Previous studies have proved that this method can better characterize the geometric shape and parameters of reservoir sand bodies, thus reflecting the superposed relationship between different sandbody [21–24]. Through the fine sedimentary microfacies research in the early stage and combined with the sedimentary mode, we found that the distributary channel is stripped in the plane and lenticular in the section with a “flat top and convex bottom”. The channel bar is elliptical in the plane and lenticular in profile with a “flat bottom and convex top”. Due to the exploration southwest of the Ordos Basin

in recent years, there is little research on the scale of the distributary channel and the channel bar in the Longdong area. Therefore, the scale of the distributary channel and the channel bar in the dense well area of the Sulige gas field is mainly used as the quantitative basis. Yang et al. carried out a geological analysis of the P₂h₈ member in the dense well area of the Su X gas field and established a reservoir geological knowledge base. It is concluded that the width of the distributary channel is 1000–2500 m [44]. Shi et al. divided the sedimentary facies of 270 wells in block Su 6 and drew the plane distribution map of sedimentary microfacies of each sand layer in combination with the plane distribution of sand bodies and the sedimentary pattern of braided rivers. It is concluded that the width of the channel bar is 600–1100 m and the length–width ratio is 1.5–2 [45]. Lei et al. obtained that the width–thickness ratio of the core beach sand body in the P₂h₈ member is 80 after the detailed comparison of well-connecting profiles and the analysis of horizontal well data in the dense well area of the Sulige gas field [46]. Based on the sedimentary background of the braided river sand body in the Pu1₂3 unit of the Daqing Oilfield, He et al. designed a sedimentary physical simulation experiment. They concluded that the width–thickness ratio of the channel bar is 80~100 and the length–width ratio is 1~3 [47]. Referring to the previous statistical information on the scale of the distributary channel and heart beach, combined with the actual statistical results of the well-connection profile and plane sedimentary microfacies distribution in the study area, some parameters corresponding to the scale of the channel sand body and heart beach in the study area are obtained as follows (Table 1).

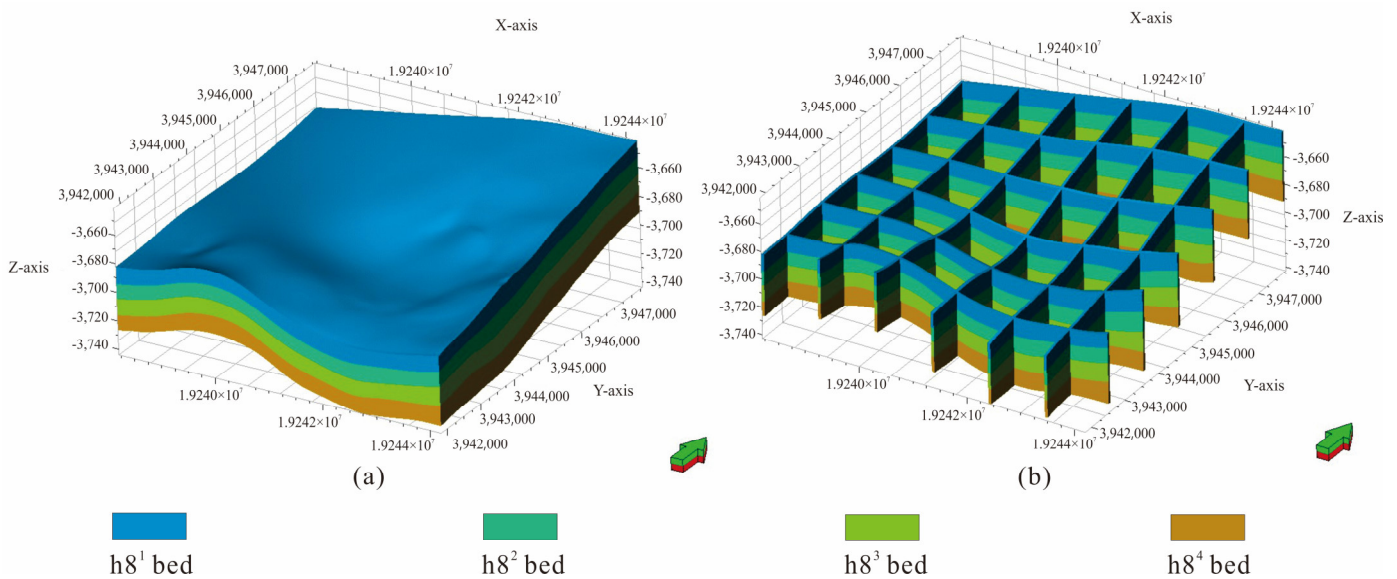


Figure 5. Simulation results of geological structure model in the study area: (a) 3D model; (b) grid model.

Table 1. Simulation parameters of sedimentary microfacies in Ct3 study area in P₂h₈ member.

Microfacies	Azimuth (°)	Width (m)	Thickness (m)	Wavelength (m)	Amplitude (m)	Length-Width Ratio
Distributary channel	20 ± 5	1500 ± 300	7 ± 5	200 ± 100	300 ± 100	/
Channel Bar	20 ± 5	600 ± 200	5 ± 3	/	/	2.5 ± 0.5

3.2.2. Sequential Indication Method

The SIS method often uses a spherical variogram, which can reflect the spatial correlation of reservoir parameters. The variogram is defined by its type, range, sill, and nugget. The range identifies the region where the variogram model approaches its plateau. The plateau is the point at which increasing the separation distance between data-point

pairs no longer increases the degree of correlation. The horizontal plane (major and minor directions) and vertical plane are frequently used for measuring variograms. The direction of the data points with the highest correlation is called the main direction, and the minor direction is defined as being perpendicular to the main direction [48]. When scaling up the sedimentary facies data on a single well, we adjust the main range, secondary range, and nugget value in the vertical, main, and secondary directions. Figure 6 shows the fitting of the variogram curve in the vertical direction, main direction, and secondary direction of microfacies of the distributary channel in the h_8^1 bed. The analysis results of the variation function of the distributary channel are shown in Table 2.

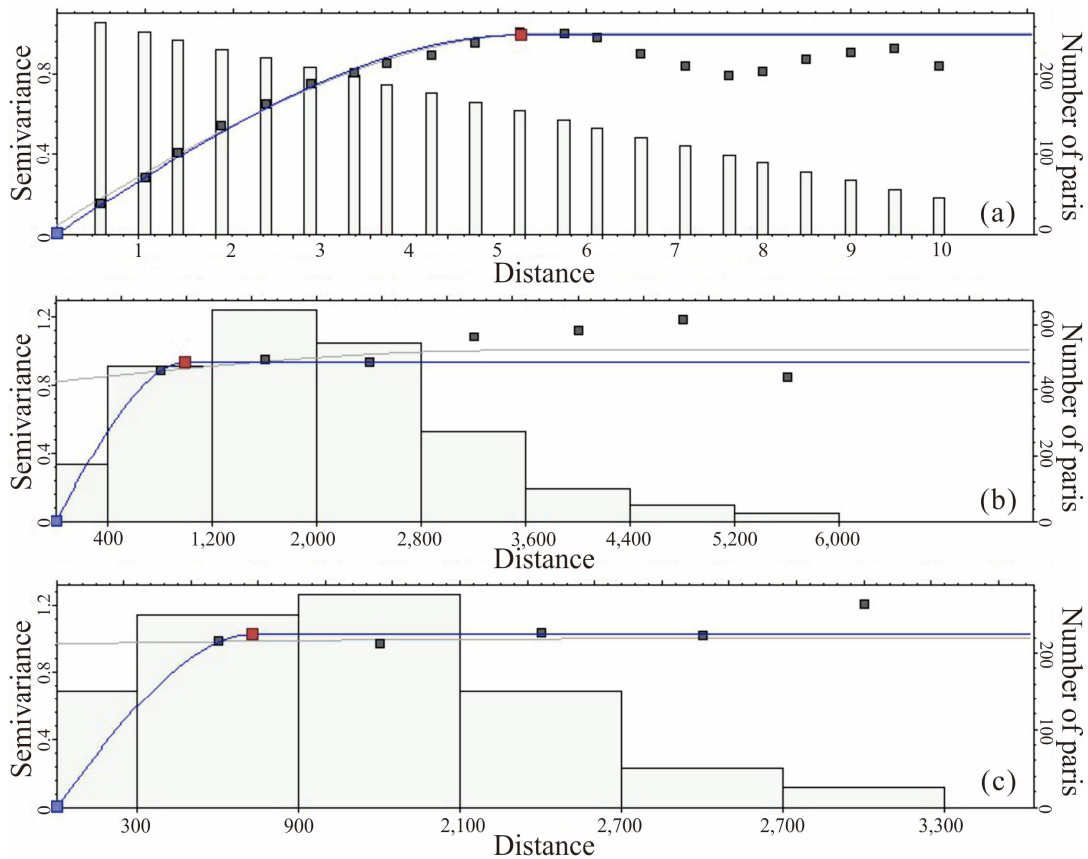


Figure 6. Scatter diagram of variation function of distributary channel microfacies in h_8^1 bed. (a) Vertical range direction; (b) main range direction; (c) secondary range direction.

Table 2. Variation function analysis results in Ct3 study area in P_2h_8 member.

Microfacies	Model Type	Vertical Range (m)	Main Range (m)	Secondary Range(m)	Azimuth (°)	Nugget	Sill
Distributary interchannel	spherical	4	900	600	30	0	1
Distributary channel	spherical	5	1000	740	30	0	1
Channel Bar	spherical	4	800	600	30	0	0.97

3.2.3. Multi-Point Geostatistics Method

The method of s2Dcd combined with DS uses 2D TIs to construct a 3D geological model. The 2D TIs include various horizontal and vertical well-connecting sections and a plane sedimentary facies diagram in the geological analysis. The 2D TIs must be perpendicular to each other because of limitations imposed by the requirements of probability fusion in the algorithm [32]. Therefore, we choose a 2D slice in the X-, Y-, and Z-directions of the 3D space. This means that the two well-connecting profiles must be orthogonal. However, in

the actual application in the work area, it is not guaranteed that all the wells selected on the well-connecting profiles are in a straight line. Additionally, it cannot be ensured that the well-connecting profile is perfectly orthogonal in both directions of the profile. Therefore, when drawing the 2D TIs of the profile, some adjustments should be made on the basis of the well-connecting profile according to the actual situation.

The source direction of the study area is northeast–southwest. We try our best to choose the wells that are in a relatively straight line and relatively orthogonal to draw the well-connecting profile in the X-direction (close to the source direction) and Y-direction (close to the vertical source direction). As the well-connecting profile does not penetrate the study area, we supplement it with reference to the plane sedimentary facies diagram and experience. The digitized well-connecting profile in the X- and Y-directions and the plane sedimentary facies figure in the Z-direction can not only aptly describe the morphology of various sedimentary microfacies and the contact relationship between them, but also match the actual geological data (Figure 7). Finally, the sedimentary facies model is obtained by using the 2D TIs in the X-, Y-, and Z-directions for 3D simulation.

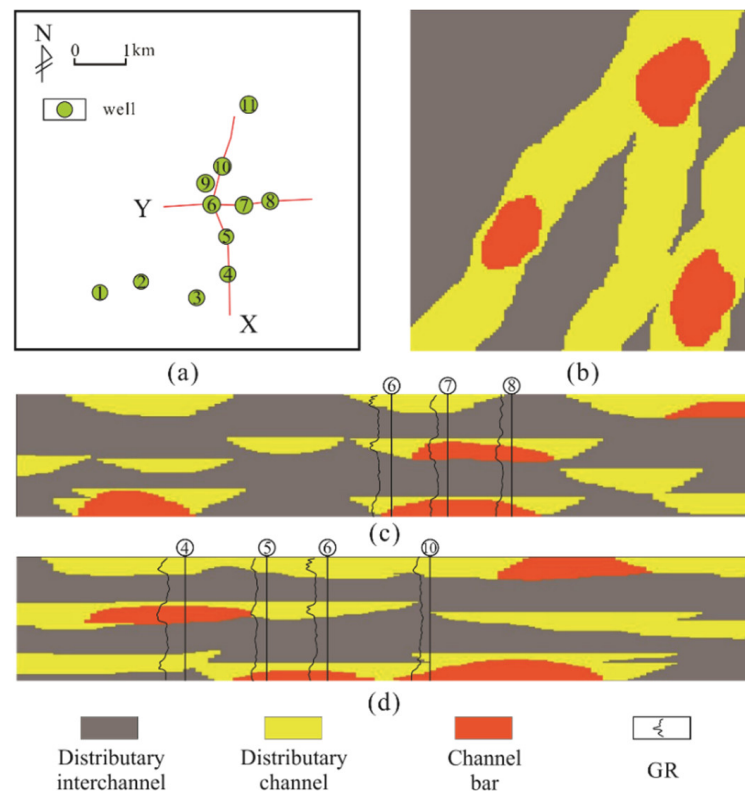


Figure 7. Digital 2D TIs. (a) Selection of the direction of TIs on the profile; (b) planar 2D TI—Z; (c) 2D TI along the source direction—X; (d) 2D TI perpendicular to the source direction—Y.

4. Results

With well data as the constraint, we set the simulation object with geometric parameters in Table 1. The distributary interchannel is used as the background facies in the simulation process to obtain the facies model (Figure 8).

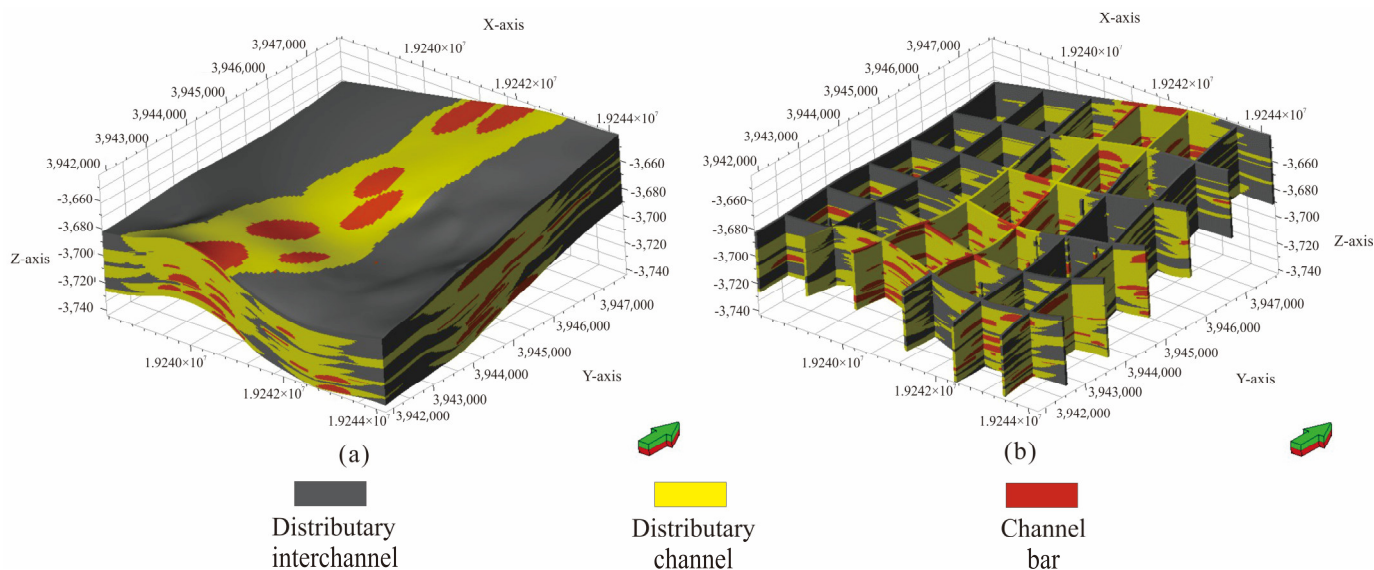


Figure 8. Simulation result of object-based method. (a) 3D model. (b) Grid model.

For example, the parameter fitting in Table 2 calculates the variogram of different microfacies. Curve fitting is carried out for each bed, and the facies model is obtained after simulation (Figure 9).

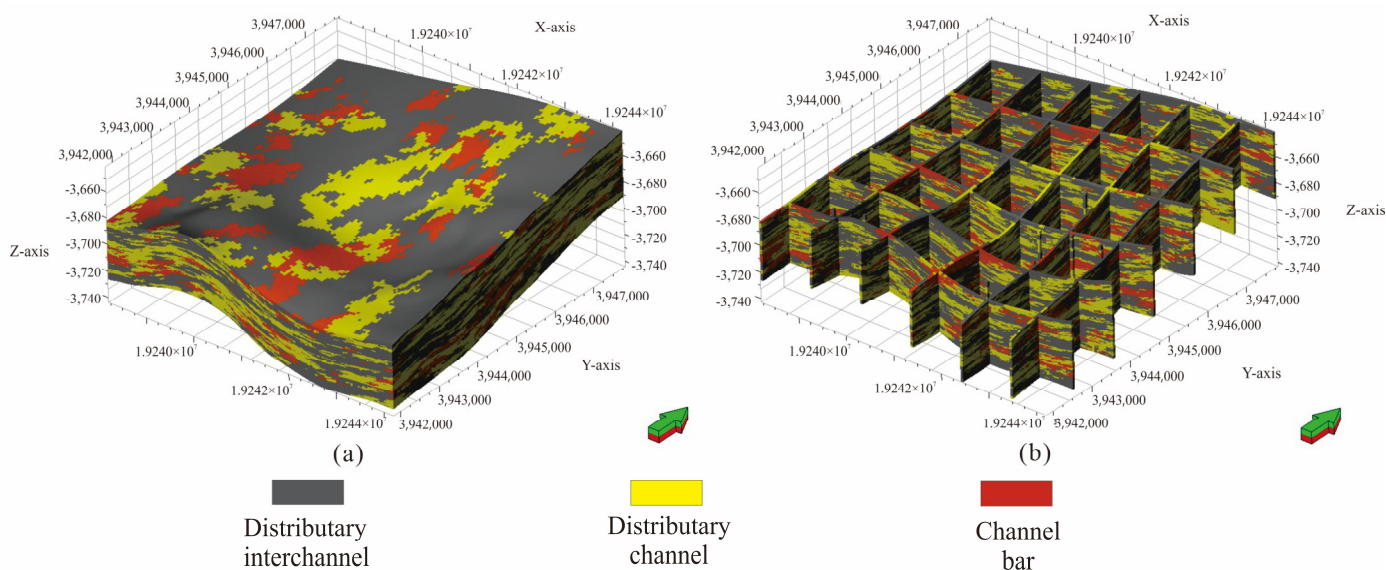


Figure 9. Simulation result of SIS. (a) 3D model; (b) grid model.

We digitized the 2D sedimentary facies map and conducted multi-point geostatistical simulation to obtain the model (Figure 10).

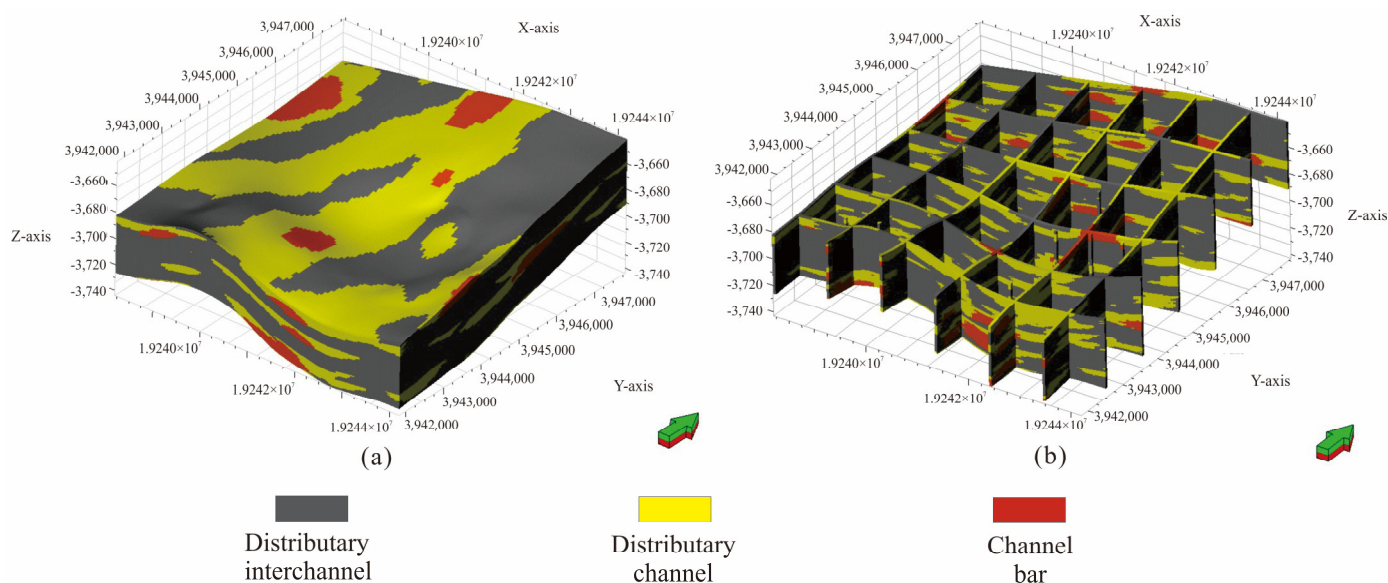


Figure 10. Simulation result of MPS based on 2D TIs. (a) 3D model; (b) grid model.

5. Discussion

Model verification is a necessary step before geological models are used to guide oil and gas production. Testing the accuracy of the model is a popular topic in the field of geological modeling in the world [4,49]. We compare and analyze the sedimentary facies models simulated by the three methods. The modeling effect is comprehensively evaluated from five aspects: Geological knowledge verification, facies proportion reproduction, well data fidelity test, well-connecting profile comparison, and comparison of the sand body thickness of the P₂h₈ member.

According to the analysis of geological data in the study area, the P₂h₈ member is a braided delta plain subfacies. Therefore, its sedimentary facies model should conform to the general understanding of geological workers for braided river reservoirs. That is, the distributary channels migrate and swing on the plane, constantly bifurcate or merge, and overlap each other vertically. The channel bar should be developed in the distributary channel. There is a certain deviation between the results of the object-based method and the actual geological understanding. It does not better simulate the spatial relationship between the channel bar and the distributary channel. In the vertical direction, the channel bar floats in the middle of the river, without contact with the bottom of the river. The physical properties of the two are usually rather different, so it is necessary to reasonably describe their spatial relationship, so as to lay the foundation for the subsequent facies-controlled reservoir attribute model. The results of SIS show that the distribution of the distributary channel and channel bar facies in the model is relatively scattered, and the channel bar is not all developed in the distributary channel (Figure 9). In general, it cannot reflect the distribution trend of fluvial facies, and the simulation effect is not ideal. It can be seen that the sedimentary facies model based on 2D TIs simulation can better describe the characteristics of braided river reservoirs (Figures 8 and 10).

Further, the facies ratio of the modeling results of the three methods is statistically analyzed (Figure 11). It can be seen that the microfacies proportion simulated by SIS is the closest to the original data. However, the simulation results of the other two methods are not very different from the original data, which shows that the three methods can achieve good simulation results in facies ratio reproduction.

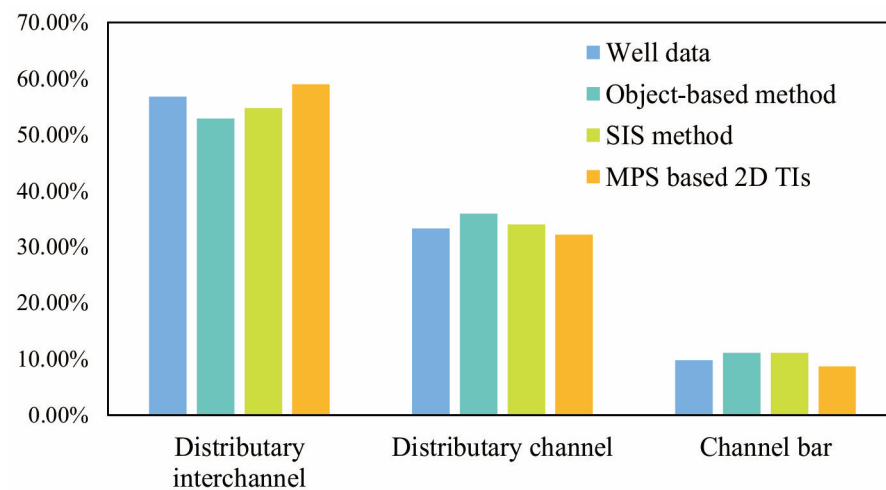


Figure 11. Facies model generated by three methods and sedimentary microfacies ratio of well data.

Figure 12 shows the fidelity of the models simulated by the three methods to the well data on the same layer plane. The object-based method cannot meet all the conditional data, which is also a difficulty for geological modelers (Figure 12a). Although the object-based method can aptly show the contact relationship between the channel bar and the distributary channel on the plane, it cannot fully match the well data, and its matching rate with the well data is only 41%. SIS is a pixel-based algorithm, which can aptly match the data (Figure 12b). The MPS based on 2D TIs is also a pixel-based simulation method, which can fully match the conditional data (Figure 12c).

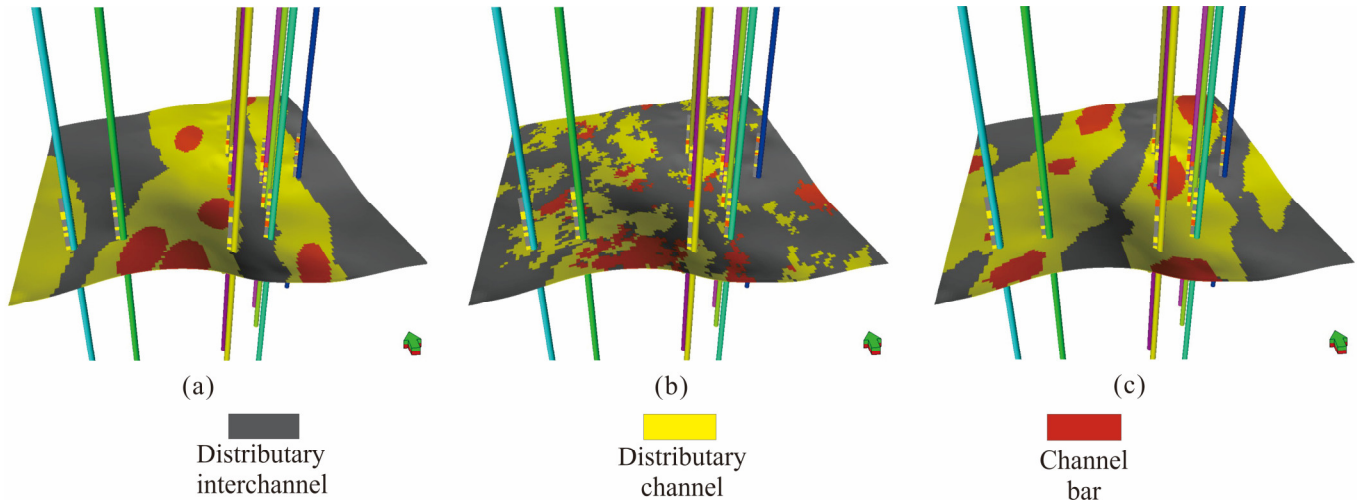


Figure 12. Comparison of facies types of the same layer between the well data and the models generated by the three methods. (a) Object-based simulation result; (b) SIS result; (c) MPS results based on 2D TIs.

In order to determine the simulation results of the three methods more intuitively, five wells with relatively close distances are selected as the well-connecting profile to compare and analyze the quality of each facies model (Figure 13). The object-based method can better display the microfacies morphology with geological cognition. However, the simulation results are inconsistent with the shape of the GR curve on the well. The SIS does not restore the geometric characteristics of the simulation object well in the vertical direction, and the facies boundary especially is relatively scattered. The MPS combining s2Dcd and DS can not only meet the various facies types indicated by the morphology of the GR curve on the well, but also show the geometric characteristics and contact relationship of the

simulation object. We compare the simulation results of the three methods from the aspects of geological knowledge verification, facies proportion reproduction, the well data fidelity test, and well-connecting profile comparison. Obviously, the MPS method based on 2D TIs combines the advantages of the object-based method and SIS and has evident advantages. Additionally, it is also proved that using 2D TIs can achieve better simulation results in the simulation of fluvial facies tight sands gas reservoirs. This study has certain theoretical value in the application of practical work areas. This method solves the problem of the difficult acquisition of 3D TI and provides a new idea and scheme for geological modeling under similar geological conditions.

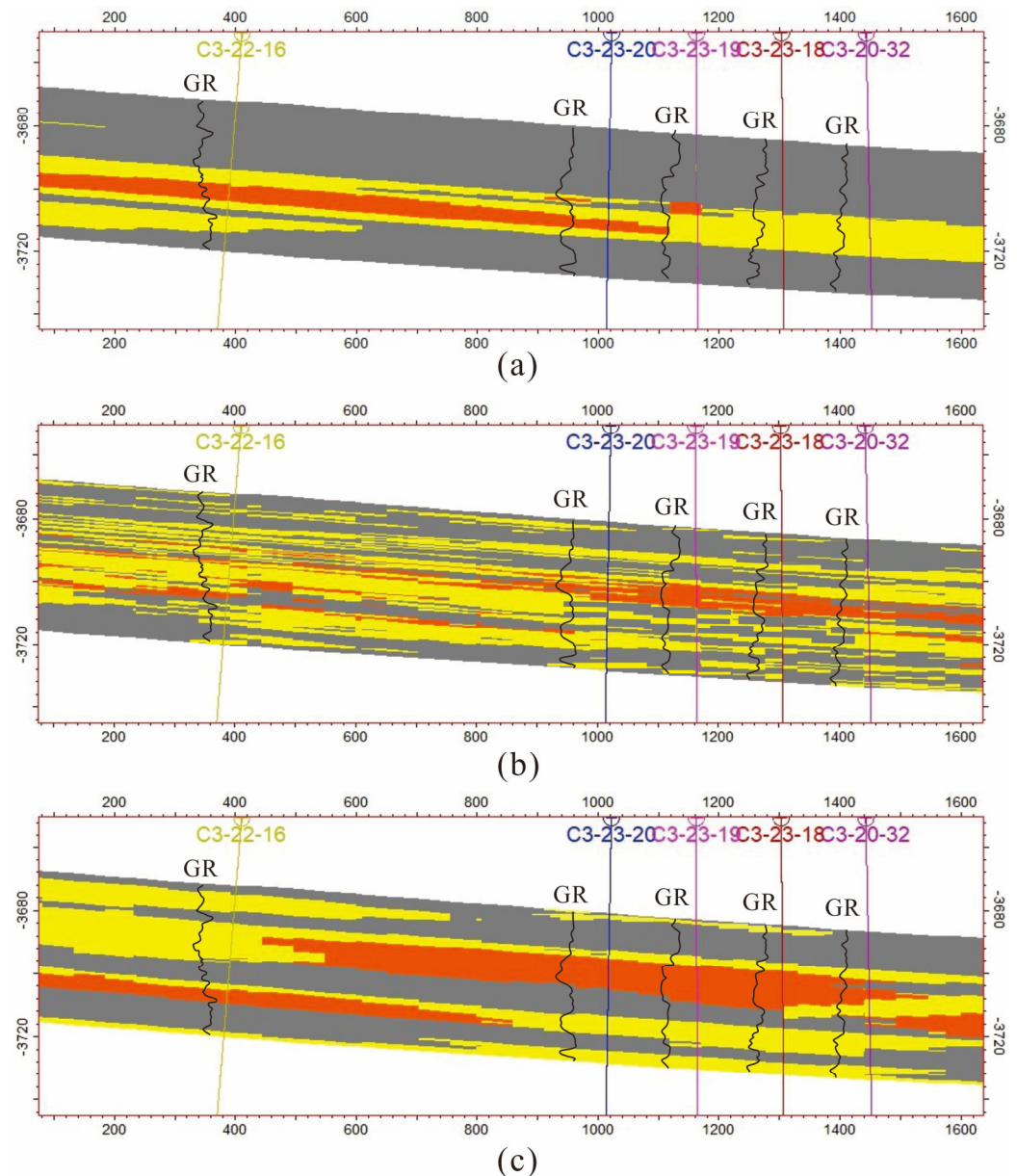


Figure 13. Comparison of simulation results of three methods and well-connecting profile. (a) Object-based simulation result; (b) SIS result; (c) MPS result based on 2D TIs.

The results of different modeling methods simulating the sandbody thickness of the P₂h₈ member are further compared. The sandstone and mudstone are divided by the amplitude of the GR curve on the well and the thickness information is obtained, which can quantitatively characterize the development form of the reservoir sandbody and the spatial distribution law of the sandbody. Then, the distribution characteristics

of sedimentary microfacies are obtained, which has a certain guiding role in judging the distribution of reservoir sand bodies. For example, the sandbody thickness distribution marked by the red box in Figure 14 shows that the simulation results of the multi-point geostatistics method based on 2D TIs are more consistent with the geological knowledge of geologists. Furthermore, the simulation results of this method can also better show the trend of river sand bodies. The relative dispersion of sand body thickness distribution using the sequential indicator method cannot show the spatial distribution characteristics of the reservoir sand body. In addition, the simulation results of the object-based method cannot fully meet the requirements of the hard data on the well, so there is no good simulation result. Based on the above five aspects of quantitative and qualitative evaluation modeling results, the method proposed in this paper can not only achieve the effect of traditional MPS simulation using 3D TI, but also outperform the sequential indication method and the object-based method under the existing conditions in this research area. The feasibility of this method in 3D geological simulation of large-scale fluvial facies tight sandstone reservoirs is verified.

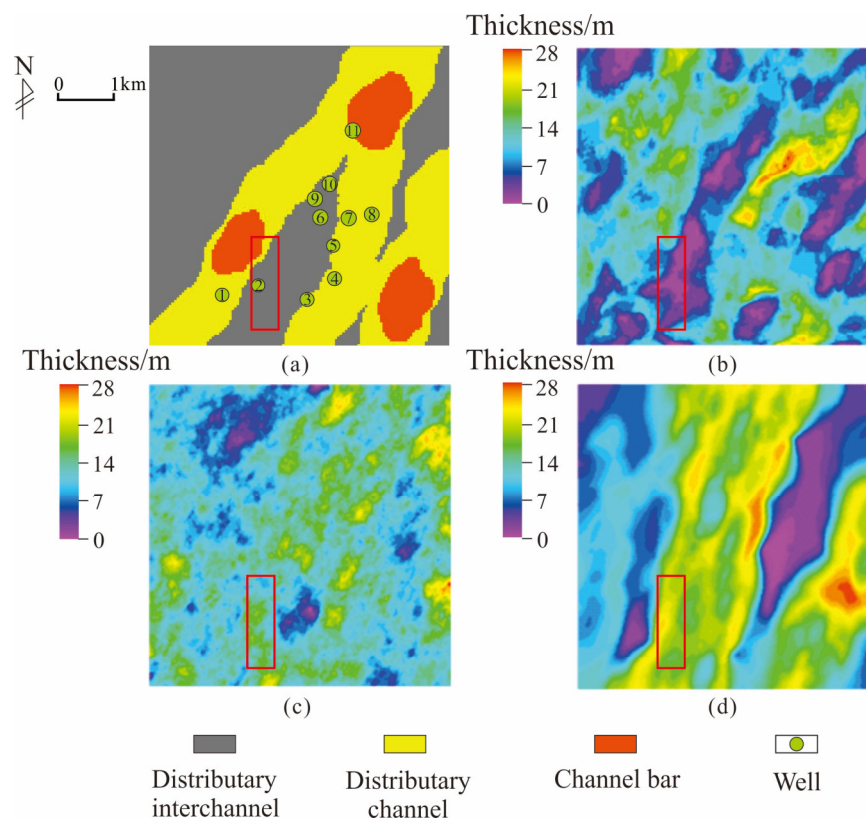


Figure 14. Thickness distribution results of sandbody in P₂h₈ member corresponding to different methods. The part of the red box clearly shows the difference of the simulation results of the three methods. (a) Distribution of plane sedimentary facies of P₂h₈ member; (b) MPS result based on 2D TIs; (c) SIS result; (d) object-based simulation result.

At present, the United States, Canada, Australia, Mexico, Venezuela, Argentina, Indonesia, China, Russia, Egypt, Saudi Arabia, and other countries and regions have carried out exploration and development research on tight gas reservoirs. Among them, the United States and Canada are the world leaders in the exploration and development of tight gas resources. So far, the most concentrated area of tight sandstone gas reservoirs is located in the Rocky Basin in North America. Some scholars have calculated the physical property data of seven typical tight sandstone gas reservoirs in North America, and 85% of the data points have overburden matrix permeability values if less than $0.1 \times 10^{-3} \mu\text{m}^2$, while approximately 10% of the data points have overburden matrix permeability values

greater than $1 \times 10^{-3} \mu\text{m}^2$ [50]. Comparing the overburden matrix permeability of tight sandstone gas reservoirs in the Ordos Basin, China, 80% of the data points are less than $0.1 \times 10^{-3} \mu\text{m}^2$ and 20% of data points are in the range of $(0.1\text{--}10) \times 10^{-3} \mu\text{m}^2$. However, there are still some data in North America with high overburden matrix permeability, which is of great significance for natural gas production. Porosity test data points of tight reservoirs in typical tight gas basins in North America are distributed in the range of 0%–26%. The measured porosity data of the Ordos Basin shows that the data points are distributed in the range of 0%–20%. This result shows that the overall low porosity and low permeability are typical features of the Ordos tight sandstone formation compared with North America. China's tight gas accounts for approximately 10% of the global resources, which has large production potential and development prospects. However, the production technology still requires further enhancement.

6. Conclusions

The Longdong area in the Ordos Basin is a tight sandstone gas reservoir. The Longdong area is identified as a braided delta plain subfacies based on core observations and logging curve characteristics. The types of sedimentary microfacies developed in this area include a distributary channel, a channel bar, and a distributary interchannel. The tight sandstone gas reservoirs of fluvial facies have strong heterogeneity. In the Ct3 study area, it is impossible to obtain 3D TIs that represent the spatial changes of underground sedimentary facies. Therefore, in this study, the MPS method was applied, which combines s2Dcd with DS and uses 2D TIs to simulate 3D models. The 2D TIs dataset includes a digital plane sedimentary facies map and vertical well-connecting profile maps. Simultaneously, the most extensively used modeling approaches, including the object-based method and the sequential indication method, were chosen to establish sedimentary facies models. Through comparative analysis, we found that although the object-based method can better display the morphology of each microfacies in the plane, it can neither depict the location relationship between the channel bar and the distributary channel in line with geological cognition in the vertical direction, nor can it fully match the well data. Although the sequential indication method can match the well data, the sand body continuity of the established model is poor. The results show that the boundary of sedimentary microfacies and the distribution of the sandbody thickness are relatively dispersed. The SIS method cannot aptly reflect the morphological characteristics of various microfacies, which is not conducive to the subsequent development of the gas reservoir. In contrast, the sedimentary facies model based on 2D TIs simulation not only matches the well data, but also better shows the morphology and contact relationship of each microfacies on the plane and profile. The results obtained by this method are consistent with the theoretical geological research results of the study area, and the prediction results of the inter-well reservoir and sandbody thickness distribution are consistent with the prior understanding of geologists. We proved that this method based on 2D TIs not only better characterizes the spatial distribution of sedimentary facies in the application of practical work areas but is also feasible in the 3D geological simulation of large-scale fluvial facies tight sandstone reservoirs. At the same time, the problem of the difficulty in obtaining 3D TI is solved. The simulation results can be used as constraints for subsequent property models.

Author Contributions: Conceptualization, S.L.; methodology, S.L.; validation, B.L.; data curation, N.Z.; writing—original draft preparation, N.Z.; writing—review and editing, S.L.; visualization, N.Z.; supervision, L.C., C.W. and J.L.; project administration, L.C., C.W. and J.L. All authors have read and agreed to the published version of the manuscript.

Funding: This research was supported by the National Natural Science Foundation of China (No. 42172172).

Data Availability Statement: All data can be obtained from the corresponding author.

Conflicts of Interest: We declare that we have no financial or personal relationships with other people or organizations that could have an inappropriate effect on our work.

References

1. Ma, X.; Jia, A.; Tan, J.; He, D. Tight sand gas development technologies and practices in China. *Pet. Explor. Dev.* **2012**, *39*, 572–579. [[CrossRef](#)]
2. Jiang, Z.; Li, Z.; Li, F.; Pang, X.; Yang, W.; Liu, L.; Jiang, F. Tight sandstone gas accumulation mechanism and development models. *Pet. Sci.* **2015**, *12*, 587–605. [[CrossRef](#)]
3. Iltaf, K.; Yue, D.; Wang, W.; Wang, X.; Li, S.; Wu, S.; Liu, R.; Zhan, W.; Mehboob, S.; Shah, S.; et al. Facies and Petrophysical Modeling of Triassic Chang 6 Tight Sandstone Reservoir, Heshui Oil Field, Ordos Basin China. *Lithosphere* **2021**, *2021*, 9230422. [[CrossRef](#)]
4. Jia, B.; Chen, Z.; Xian, C. Investigations of CO₂ storage capacity and flow behavior in shale formation. *J. Pet. Sci. Eng.* **2022**, *208*, 109659. [[CrossRef](#)]
5. Wang, X.; Hou, J.; Li, S.; Dou, L.; Song, S.; Kang, Q.; Wang, D. Insight into the nanoscale pore structure of organic-rich shales in the Bakken Formation, USA. *J. Pet. Sci. Eng.* **2020**, *191*, 107182. [[CrossRef](#)]
6. Rokanuzzaman, M.; Veawab, A.; Aroonwilas, A. Design method for layered-bed adsorption column for separation of CO₂ and N₂ from natural gas. *Energy Procedia* **2017**, *114*, 2441–2449.
7. Jia, A.; Wei, Y.; Guo, Z.; Wang, G.; Meng, D.; Huang, S. Development status and prospect of tight sandstone gas in China. *Natural Gas Industry* **2022**, *42*, 83–92.
8. Reng, P. *Reservoir Characteristics and Geological Modeling of the upper He8 Reservoir in the Tao2 Area in Sulige Gas Field*; Xi'an Shiyou University: Xi'an, China, 2015.
9. Zhang, C.; Li, J.; Liu, R. Microscopic characteristics and forming mechanisms of He 8th member tight sandstone gas reservoirs in Ordos Basin. *China Pet. Explor.* **2019**, *24*, 476–484.
10. Jia, C.; Zheng, M.; Zhang, Y. Unconventional hydrocarbon resources in China and the prospect of exploration and development. *Petr. Explor. Dev.* **2012**, *39*, 139–146. [[CrossRef](#)]
11. Yang, H.; Fu, J.; Liu, X.; Meng, P. Accumulation conditions and exploration and development of tight gas in the Upper Paleozoic of the Ordos Basin. *Petr. Explor. Dev.* **2012**, *39*, 315–324. [[CrossRef](#)]
12. Li, J.; Wang, Y.; Zhao, J.; Li, L.; Zheng, J.; Hu, W. Accumulation patterns of natural gas in the Upper Paleozoic in Longdong area, Ordos Basin. *Oil Gas Geol.* **2016**, *37*, 180–188.
13. Shan, J.; Zhang, B.; Zhao, Z.; Li, F.; Wang, H.; Wang, B. Single stage and sedimentary evolution process analysis of braided river—A case from Su X block of western Sulige gas field in Ordos Basin. *Acta Petrol. Sin.* **2015**, *33*, 773–785.
14. Zhu, S.; Cui, H.; Chen, J.; Luo, G.; Wang, W.; Yang, Y.; Shi, L. Sedimentary system and sandstone reservoir petrology of a shallow water delta: Case study of the Shan-1 and He-8 members in the western Ordos Basin. *Acta Petrol. Sin.* **2021**, *39*, 126–139.
15. Wu, S. *Reservoir Characterization and Modeling*, 1st ed.; Petroleum Industry Press: Beijing, China, 2010; pp. 45–46.
16. Liang, B.; Liu, Y.; Shao, Y.; Wang, Q.; Zhang, N.; Li, S. 3D Quantitative Characterization of Fractures and Cavities in Digital Outcrop Texture Model Based on Lidar. *Energies* **2022**, *15*, 1627. [[CrossRef](#)]
17. Li, S.; Yin, Y.; Zhang, C. *A Series of Techniques for Reservoir Stochastic Modeling*, 1st ed.; Petroleum Industry Press: Beijing, China, 2007; pp. 8–9.
18. Wu, S.; Li, W. Multiple-point geostatistics: Theory, application and perspective. *J. Palaeogeogr.* **2005**, *7*, 137–144.
19. Wang, J.; Zhang, T. *Stochastic Modeling of Oil and Gas Reservoir*, 1st ed.; Petroleum Industry Press: Beijing, China, 2001; pp. 11–12.
20. Wang, X.; Yu, S.; Li, S.; Zhang, N. Two parameter optimization methods of multi-point geostatistics. *J. Pet. Sci. Eng.* **2022**, *208*, 109724. [[CrossRef](#)]
21. Huo, C.; Li, G.; Zhao, C.; Yan, W.; Yang, Q. Integrated reservoir geological modeling based on seismic, log and geological data. *Acta Petrol. Sin.* **2007**, *28*, 66–71.
22. Jones, T. Using flowpaths and vector fields in object-based modeling. *Comput. Geosci.* **2001**, *27*, 33–138. [[CrossRef](#)]
23. Chen, Z.; Osadetz, K.; Gao, H.; Hannigan, P. SuperSD: An object-based stochastic simulation program for modeling the locations of undiscovered petroleum accumulations. *Comput. Geosci.* **2004**, *30*, 281–290. [[CrossRef](#)]
24. Zhou, F.; Shields, D.; Tyson, S.; Tyson, S.; Esterle, J. Comparison of sequential indicator simulation, object modelling and multiple-point statistics in reproducing channel geometries and continuity in 2D with two different spaced conditional datasets. *J. Pet. Sci. Eng.* **2018**, *166*, 718–730. [[CrossRef](#)]
25. Jones, R.; Mccaffrey, K.; Imber, J.; Wightman, R.; Smith, F.; Holdsworth, E.; Clegg, P.; Paola, D.; Healy, D.; Wilson, W. Calibration and validation of reservoir models: The importance of high resolution, quantitative outcrop analogues. *Geol. Soc. Spec. Publ.* **2008**, *309*, 97–98. [[CrossRef](#)]
26. Enge, H.; Buckley, S.; Rotevatn, A.; Howell, J. From outcrop to reservoir simulation model: Workflow and procedures. *Geosphere* **2007**, *3*, 469–490. [[CrossRef](#)]
27. Shi, S.; Hu, S.; Feng, W.; Liu, W. Building geological knowledge database based on google earth software. *Acta Petrol. Sin.* **2012**, *30*, 869–878.
28. Yan, B.; Zhang, X.; Yu, L.; Zhang, D.; Jiang, G.; Yang, Y.; Sun, y.; Han, X.; Xu, Y. Point bar configuration and residual oil analysis based on core and dense well pattern. *Petr. Explor. Dev.* **2014**, *41*, 654–662. [[CrossRef](#)]
29. Zhang, W.; Duan, T.; Zheng, L. Generation and application of three-dimensional MPS training images based on shallow seismic data. *Oil Gas Geol.* **2015**, *36*, 1030–1037.

30. Okabe, H.; Blunt, M. Pore space reconstruction of vuggy carbonates using microtomography and multiple-point statistics. *Water Resour. Res.* **2007**, *43*, 179–183. [[CrossRef](#)]
31. Comunian, A.; Renard, P.; Straubhaar, J. 3D multiple-point statistics simulation using 2D training images. *Comput. Geosci.* **2012**, *40*, 49–65. [[CrossRef](#)]
32. Mariethoz, G.; Renard, P. Reconstruction of Incomplete Data Sets or Images Using Direct Sampling. *Math. Geosci.* **2010**, *42*, 245–268. [[CrossRef](#)]
33. Gueting, N.; Caers, J.; Comunian, A.; Vanderborght, J.; Englert, A. Reconstruction of three-dimensional aquifer heterogeneity from two-dimensional geophysical data. *Math. Geosci.* **2018**, *50*, 53–75. [[CrossRef](#)]
34. Fu, B.; Shi, L.; Jiang, L.; Du, P.; Chen, S.; Bai, Z. Application of multiple-point geostatistics method in reservoir modeling of tight sandstone gas reservoir: Taking block s48-17-64 as an example. *Fault-Block Oil Gas Field* **2014**, *21*, 726–729.
35. Cao, B.; Luo, X.; Zhang, L.; Lei, Y.; Zhou, J. Petrofacies prediction and 3-D geological model in tight gas sandstone reservoirs by integration of well logs and geostatistical modeling. *Mar. Pet. Geol.* **2019**, *114*, 104202. [[CrossRef](#)]
36. Liu, H.; Qin, Z.; Xu, L.; Wang, F.; Tong, Q.; Lin, J.; Yin, S.; Wang, W. Distribution of shallow water delta sand bodies and the genesis of thick layer sand bodies of the Triassic Yanchang Formation, Longdong Area, Ordos Basin. *Pet. Explor. Dev.* **2021**, *48*, 123–135. [[CrossRef](#)]
37. He, J.; Zhu, X.; Li, M.; Liu, F.; Ye, L.; Xue, M. Parent rock types and tectonic setting of the Permian Shanxi and Shihezi Formations in Longdong area, Ordos Basin. *J. Palaeogeogr.* **2017**, *19*, 285–288.
38. He, S.; Lan, Z.; Men, C. New braided river model in Sulige Gas Field of Ordos Basin. *Acta Petrol. Sin.* **2005**, *26*, 25–29.
39. Zheng, Q.; Liu, Q.; Liang, X.; Zhang, J.; Zhang, J.; Liu, T. Sedimentary facies distribution characteristics of Chang 4 + 5 reservoir in Longdong area, Ordos Basin. *Lithol. Reserv.* **2019**, *31*, 26–35.
40. Xiao, H.; Liu, R.; Zhang, F.; Lin, C.; Zhang, M. Sedimentary model reconstruction and exploration significance of Permian He 8 Member in Ordos Basin, NW China. *Petr. Explor. Dev.* **2019**, *46*, 268–280. [[CrossRef](#)]
41. Wang, Q.; Wang, F.; Wei, Y.; Zhang, L.; Fang, Y. Dimentary facies of sub oil-bearing formation of Chang 81 and their influence on physical properties of reservoir, Heshui, Ordos Basin, NW China. *Sediment. Geol. Tethyan Geol.* **2021**, *41*, 88–99.
42. Li, L.; Zhao, Y.; Ma, C.; Jin, S.; Zhao, Y.; Yang, L. Patterns and Methods of Sandy Braided-River Island and Channel Sand Identification. *Spec. Oil Gas Reserv.* **2020**, *27*, 63–69.
43. Cui, G.; Wei, Q.; Xiao, L.; Wang, S.; Hu, R.; Wang, C. Reservoir Characteristics of Permian Lower He 8 Member in Longdong Area, Ordos Basin. *Geoscience* **2021**, *35*, 1088–1097.
44. Yang, T.; Wang, J.; Wang, Y.; Fu, B.; Xue, W.; Hao, Q. Reservoir modeling of tight sandstone gas reservoir based on geological knowledge database: A case from Su X block in Sulige gas field. *Lithol. Reserv.* **2017**, *29*, 138–145.
45. Shi, S.; Gao, L.; Liu, L.; Gu, J.; Bi, M. Geological modeling of effective sandstone reservoir of the Su-6 infilling drilling pilot in Sulige Gas Field. *J. Southwest Petr. Univ. (Sci. Technol. Ed.)* **2015**, *37*, 44–50.
46. Lei, B.; Li, Y.; Li, F.; Zhao, Z.; Zhu, Y.; Zhang, Z. Sedimentary microfacies and sandbody distribution of the Member 8 of Xiashihezi formation in horizontal well zone, central Sulige area, Ordos Basin. *J. Palaeogeogr.* **2015**, *17*, 91–105.
47. He, Y.; Song, B.; Zhang, C. A study of braided river sand deposition Chang yuan, Daqing through physical simulation experiments. *Earth Sci. Front.* **2012**, *19*, 41–48.
48. Pyrcz, M.; Deutsch, C. *Geostatistical reservoir modeling*, 1st ed.; Oxford university press: New York, NY, USA, 2014; pp. 56–57.
49. Li, X.; Yuan, J.; Li, K. Reservoir modeling research and method optimization in T2111 reservoir of MOXI gasfield. *Nat. Gas Pet. Explor. Dev.* **2008**, *31*, 5–8+26+81.
50. Li, Y.; Song, Y.; Jiang, Z.; Wang, P.; Zhao, R.; Liu, S.; Y, L. Parameters statistic analysis of global tight sand gas basins. *Nat. Gas Geosci.* **2017**, *28*, 952–964.